Acute Hyperglycemia Increases Brain Pregenual Anterior Cingulate Cortex Glutamate Concentrations in Type 1 Diabetes

Nicolas R. Bolo,[1,2] Alan M. Jacobson,[3] Gail Musen,[2,4] Matcheri S. Keshavan,[1,2] and Donald C. Simonson[5]

The brain mechanisms underlying the association of hyperglycemia with depressive symptoms are unknown. We hypothesized that disrupted glutamate metabolism in pregenual anterior cingulate cortex (ACC) in type 1 diabetes (T1D) without depression affects emotional processing. Using proton MRS, we measured glutamate concentrations in ACC and occipital lobe cortex (OCC) in 13 subjects with T1D without major depression (HbA$_{1c}$ 7.1 ± 0.7% [54 ± 7 mmol/mol]) and 11 healthy control subjects without diabetes (HbA$_{1c}$ 5.5 ± 0.2% [37 ± 3 mmol/mol]) during fasting euglycemia followed by a 60-min +5.5 mmol/L hyperglycemic clamp (HG). Intrinsic neuronal activity was assessed using resting-state blood oxygen level–dependent functional MRI to measure the fractional amplitude of low-frequency fluctuations in slow-4 band (fALFF4). Emotional processing and depressive symptoms were assessed using emotional tasks (emotional Stroop task, self-referent encoding task [SRET]) and clinical ratings (Hamilton Depression Rating Scale [HAM-D], Symptom Checklist-90 Revised [SCL-90-R]), respectively. During HG, ACC glutamate increased (1.2 mmol/kg, 10% $P = 0.014$) while ACC fALFF4 was unchanged (-0.007, -2%, $P = 0.449$) in the T1D group; in contrast, glutamate was unchanged (-0.2 mmol/kg, -2%, $P = 0.578$) while fALFF4 decreased (-0.05, -13%, $P = 0.002$) in the control group. OCC glutamate and fALFF4 were unchanged in both groups. T1D had longer SRET negative word response times ($P = 0.017$) and higher depression rating scores (HAM-D $P = 0.020$, SCL-90-R depression $P = 0.008$). Higher glutamate change tended to associate with longer emotional Stroop response times in T1D only. Brain glutamate must

be tightly controlled during hyperglycemia because of the risk for neurotoxicity with excessive levels. Results suggest that ACC glutamate control mechanisms are disrupted in T1D, which affects glutamatergic neurotransmission related to emotional or cognitive processing. Increased prefrontal glutamate during acute hyperglycemic episodes could explain our previous findings of associations among chronic hyperglycemia, cortical thinning, and depressive symptoms in T1D.

The prevalence of comorbid depression in adults with type 1 diabetes (T1D) is about three times higher than in populations without diabetes (1,2). The etiology of depression can be multifactorial, with biological as well as environmental factors contributing to depressive symptoms. There is a well-established association between hyperglycemia and depression (3–5), but the potential biological mechanisms underlying this association are unknown. Since the brain is almost entirely dependent on glucose for its energy and neurotransmission needs, hyperglycemia could impact brain function directly by a mechanism that is independent of environmental stressors. A better understanding of the brain biological mechanisms relating hyperglycemia to depressive symptoms could help to develop better treatments of depression in T1D.

Glucose is the brain's main energy source, and it also provides brain cells with precursors for synthesis of the main excitatory and inhibitory neurotransmitters glutamate and γ-aminobutyric acid (GABA), respectively. Glutamate is released by ~90% of the brain's neurons during excitation (6), and glutamatergic neurotransmission underlies synaptic

---

[1]Department of Psychiatry, Beth Israel Deaconess Medical Center, Boston, MA
[2]Department of Psychiatry, Harvard Medical School, Boston, MA
[3]Research Institute, NYU Long Island School of Medicine, Mineola, NY
[4]Research Division, Joslin Diabetes Center, Boston, MA
[5]Division of Endocrinology, Diabetes, and Hypertension, Brigham and Women's Hospital, Harvard Medical School, Boston, MA

Corresponding author: Nicolas R. Bolo, nbolo@bidmc.harvard.edu

plasticity (7–9), development (10), and learning (11,12). During normal glutamatergic neurotransmission, after glutamate is released in the synaptic cleft for interaction with ionotropic and metabotropic glutamate receptors, it is cleared from the synaptic space by astrocytic reuptake for recycling. The glutamate in astrocytes is converted to glutamine that is transferred back to neurons and converted back to glutamate for incorporation to neuronal glutamatergic vesicles and new release. This cycle constitutes the glutamate-glutamine cycle (13). In healthy adults, the brain glutamate pool is thus tightly regulated by a homeostatic mechanism to avoid excessive activity at glutamate receptors, which can ultimately result in excitotoxicity or neuronal cell death (14).

MRS is a technique that allows noninvasive assessment of brain metabolites, including the glutamatergic metabolites glutamate, glutamine, and combined glutamate plus glutamine (Glx) as well as other metabolites of interest to brain cellular metabolism such as glucose, the neuronal marker N-acetylaspartate (NAA), and the total creatine plus phosphocreatine (TCr) related to regeneration of ATP (15). MRS has been used to assess glutamatergic metabolites in T1D (16) as well as in various psychiatric disorders, including depression (17). Blood oxygen level–dependent (BOLD) functional MRI (fMRI) is a technique that allows assessment of regional intrinsic brain activity, activation in response to cognitive and emotional tasks, or functional connectivity. It has been used to show functional alterations in both T1D (18,19) and depression (20).

Alterations of glutamatergic neurotransmission are implicated in the pathophysiology of depression, and the glutamatergic system constitutes a recent target for antidepressant medications (21,22). The relationship between brain glutamatergic metabolite concentrations and major depressive disorder (MDD) is unclear, with some MRS studies showing decreased (21), others increased (23), and yet others unchanged (24) glutamate or Glx levels compared with control. These discrepancies are likely due to differences in brain regional location of MRS measurements and medication status. Also, brain glutamate concentrations measured during resting steady state may not accurately reflect anomalies in glutamatergic metabolism or glutamate regulation by homeostatic mechanisms, which might better be revealed by comparison of levels between two different physiologically controlled states.

We previously showed in a large T1D population that increased glycosylated hemoglobin (HbA$_{1c}$) is associated with increased pregenual anterior cingulate cortex (ACC) glucose and combined glutamate-glutamine-GABA, which in turn is associated with increased clinical depressive symptom scores and decreased cognitive scores (16). We also showed that there was cortical thinning in superior prefrontal cortex regions, which was associated with lifetime average HbA$_{1c}$ and was more extensive in T1D with comorbid depression (25). The ACC is a critical part of the brain's associative emotional processing network, involved in self-reflective emotional awareness and emotional evaluation of internal proprioception and external sensory input for decision making (26). Alterations of ACC functional activity and connectivity are implicated in depression (27,28) and may play a causal role in negative affect and cognitive control (29). A study of brain metabolites in T1D using MRS during hyperglycemia showed that glutamate and NAA levels were lower in occipital lobe gray matter compared with control, suggesting a partial neuronal loss or dysfunction as a consequence of long-term T1D (30). A more recent MRS study showed increased glutamate levels during euglycemia in a periventricular region compared with control, which correlated with glycemic control, suggesting a potential role for glutamate as an early marker of hyperglycemia-induced cerebral complications of T1D (31). Using BOLD fMRI during hypoglycemia, we have shown that activation in response to a working memory task is increased and deactivation decreased in subjects with T1D compared with control subjects without diabetes with equal task performance levels, suggesting reduced cerebral efficiency in T1D (18). In another BOLD fMRI study using a psychomotor speed task, higher HbA$_{1c}$ was associated with longer response times (worse performance) and higher activation in sensorimotor, frontal, and cingulate cortex regions, and higher frontal and subcortical activation was associated with longer response times. However, higher activation in the superior parietal lobule was associated with shorter response times, suggesting that increased parietal activation might compensate for frontal dysregulation in brain activation in the presence of hyperglycemia (32).

In the current study, we investigated the effect of an experimentally controlled acute episode of hyperglycemia on ACC glutamate levels in patients with T1D without clinical depression. To investigate the regional specificity of our findings, we also performed MRS in the occipital lobe cortex (OCC), selecting a region encompassing the primary sensory visual area V1. We evaluated emotional function using computerized versions of the emotional Stroop task and self-referent encoding task (SRET), and we evaluated depressive symptoms by using clinical depression rating scores. Our primary hypothesis was that glutamate would be increased specifically in the ACC during acute hyperglycemia in T1D. We also examined effects on NAA as a control metabolite. To better understand the potential relationship among glutamatergic metabolism, neurotransmission, and depressive symptoms, we further explored effects on measures of intrinsic neuronal activity and emotional processing as well as effects on other metabolites related to glutamate and neuronal mitochondrial energetics (Glx and TCr).

RESEARCH DESIGN AND METHODS

The study was conducted according to the principles of the Declaration of Helsinki. The protocol was approved by the institutional review board of the Beth Israel Deaconess Medical Center (BIDMC). All subjects gave voluntary informed written consent before participation.

Subjects

The study sample consisted of 13 volunteers with T1D (nine women, four men), with a mean ± SD age of 25 ± 4 years, HbA$_{1c}$ of 7.1 ± 0.7% (54 ± 7 mmol/mol), age at onset of 12 ± 6 years, and diabetes duration of 13 ± 6 years, and 11 healthy control volunteers without diabetes (five women, six men), with a mean age of 27 ± 7 years and HbA$_{1c}$ of 5.5 ± 0.2% (37 ± 3 mmol/mol) (Table 1). Subjects were excluded from either group if they had clinically significant cardiovascular, neurologic, or Axis I psychiatric disease (notably, current or an antecedent episode of MDD); malignancy; drug or alcohol abuse; any contraindications to MRI, such as metallic implants, pregnancy, or claustrophobia; if they were taking any type of antidepressant medication; or if they were heavy smokers according to the Epidemiology of Diabetes Interventions and Complications (EDIC) scale (33). Patients with 10–25 years' diabetes duration were included in the T1D group. All study procedures were performed at the Clinical Research Center and MRI Research Center of BIDMC. After the screening visit to determine inclusion criteria, all subjects came to BIDMC in the morning for an MRI/MRS study visit.

Hyperglycemic and Euglycemic Clamps

The study protocol is shown in Fig. 1 and described below. All studies were performed between 0800 and 1300 h after an overnight fast. The clamp technique is described in detail elsewhere (19,34) and briefly summarized here. An intravenous catheter was inserted into an antecubital vein for the administration of dextrose and/or insulin, and a second catheter was inserted into a distal forearm or hand vein for the withdrawal of blood samples. A heated gel pack was used to warm the hand to arterialize the

venous blood. During the entire clamp protocol, glucose levels were measured every 5 min, and insulin was measured every 10 min. Plasma glucose was measured by the glucose oxidase method, and insulin was measured by ELISA.

During the study visit, MRI/MRS was performed during a fasting euglycemic state (EU) followed by a hyperglycemic clamp (HG). During a baseline period before scanning, only subjects with T1D received a low-dose insulin infusion to reduce their plasma glucose to a euglycemic level. MRI/MRS was first performed during the EU period. At the beginning of EU (time = 0) and during the entire experiment, subjects with T1D received a constant insulin infusion at a rate of 0.25 mU/kg/min to control plasma glucose levels. Control subjects did not receive any infusion during EU. All subjects then exited the scanner to begin dextrose infusion for the HG. After 30 min, when individual plasma glucose levels were stabilized at the target level of 5.5 mmol/L above the EU level, subjects were repositioned in the scanner, and MRI/MRS was repeated during 60 min of the HG period.

MRI and MRS Data Acquisition

MRI and MRS data were acquired using a 3T Signa HDxt MRI scanner (LX 15.0; GE Healthcare, Chicago, IL) with an 8-channel proton head coil. We acquired T1-weighted structural images using a magnetization prepared rapid acquisition gradient echo acquisition sequence with repetition time (TR)/echo time (TE) = 7,000/3 ms, two averages, flip angle 8°, in-plane matrix size = 256 × 256, field of view = 25.6 cm, slice thickness = 1.6 mm, 124 sagittal slices, fat saturation, inversion recovery inversion time = 650 ms, and bandwidth = 31.25 kHz. Structural images

Table 1—Demographics, clinical characteristics, and depression and cognition rating scores of subjects

Characteristic	T1D (n = 13)	Control (n = 11)	P*
HbA$_{1c}$ (%)	7.1 ± 0.7 (6.0–8.0)	5.5 ± 0.2 (5.1–6.0)	**<0.0001**
HbA$_{1c}$ (mmol/mol)	54 ± 7 (42–64)	37 ± 3 (32–42)	**<0.0001**
Age (years)	25 ± 4 (19–33)	27 ± 7 (21–45)	0.450
Diabetes onset age (years)	12 ± 6 (4–20)	—	—
Diabetes duration (years)	13 ± 6 (5–23)	—	—
Sex (female/male)	9/4	5/6	0.238
HAM-D rating score	1.8 ± 1.9 (0–6)	0.3 ± 0.4 (0–1)	**0.017**
SCL-90-R depression rating score	7.3 ± 6.9 (2–23)	1.1 ± 1.5 (0–5)	**0.008**
Years of education	16 ± 2 (14–20)	17 ± 2 (15–20)	0.369
WASI IQ	123 ± 9 (109–139)	120 ± 8 (104–129)	0.351
D-KEFS trail making (s)	66 ± 18 (46–116)	56 ± 17 (36–75)	0.186
D-KEFS verbal fluency score	46 ± 9 (23–55)	51 ± 11 (36–75)	0.213
WMS VPA 1 immediate score	39 ± 9 (23–55)	36 ± 8 (28–52)	0.360
WMS VPA 2 delayed score	12 ± 3 (6–14)	12 ± 2 (8–14)	0.983
Grooved Pegboard dominant hand (s)	61 ± 9 (45–84)	60 ± 8 (50–75)	0.704
Grooved Pegboard nondominant hand (s)	66 ± 11 (43–89)	68 ± 9 (53–78)	0.655

Data are mean ± SD (range) and n. P values < 0.05 appear in boldface type. WMS VPA, Wechsler Memory Scale Verbal Paired Associates subtest. *By one-way ANOVA t test.
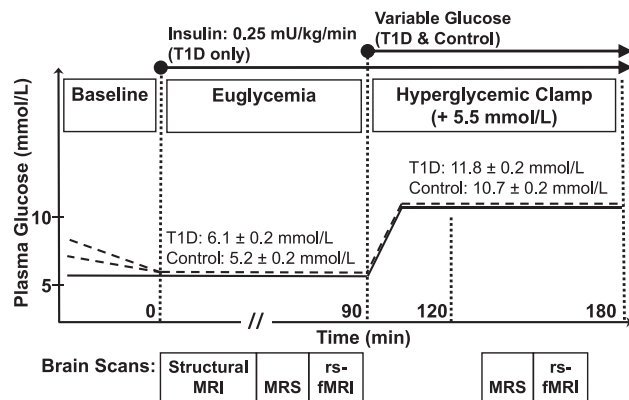
Figure 1—Experimental protocol. Plasma glucose levels vs. experiment time. Dotted lines represent subjects with T1D, and solid lines represent control subjects. During baseline, subjects with T1D received a low-dose insulin infusion to reduce their plasma glucose to euglycemia. An EU period was followed by an HG period. At the beginning of EU (time = 0) and during the entire experiment, subjects with T1D received a constant basal insulin infusion at 0.25 mU/kg/min. After EU scans, all subjects exited the scanner to initiate the HG period with a primed variable glucose infusion to attain a target increase in glycemic level of 5.5 mmol/L. Subjects were repositioned in the scanner when plasma glucose levels had stabilized at the EU +5.5 mmol/L level for the HG scanning period. Scans were performed during each of the two plasma glucose conditions, indicated by boxes beneath each plot. The mean ± SE values of plasma glucose are indicated for each visit and condition for the T1D and control groups.

were used for accurate MRS voxel positioning according to brain structural landmarks and for determination of partial volume fractions of gray and white matter and cerebrospinal fluid in the MRS voxel. The partial volume fractions were used for absolute quantitation of metabolites in MRS data analyses. We acquired single-voxel MRS using the point-resolved spectroscopy sequence with TR/TE = 2,000/35 ms, 5 kHz spectral width, 4,096 complex points, and 128 averages in two volumes of $2 \times 2 \times 2$ cm^3 (8 mL) positioned in the pregenual ACC and OCC centered on the calcarine fissure (see Fig. 2). The ACC voxel contained mostly pregenual ACC gray matter but also some medial prefrontal cortex. For each water-suppressed metabolite MRS signal acquisition, we acquired the nonsuppressed water signal (with 16 averages) in the same voxel to be used as a quantitation reference for water scaling (35,36). We acquired BOLD resting-state fMRI (rs-fMRI) using a gradient-echo echo-planar imaging sequence with TR/TE = 2,000/25 ms, flip angle 90°, in-plane matrix size = 64×64, field of view = 24×24, and axial slice thickness = 4 mm with 1-mm gap; 180 whole-head volumes were acquired for an fMRI run duration of 6 min. During fMRI, subjects were instructed to keep their eyes open and to look at a white cross on a black background, which was visualized through a mirror placed on the head coil.

To limit motion artifacts in the acquired data, we made all efforts to ensure that subjects were as comfortable as possible in the scanner, using blankets and foam pillows and placing foam pads alongside the head inside the head coil to limit head motion. Subjects were frequently questioned about any discomfort or concerns, and none were reported. None of the studies needed to be interrupted because of physical or psychological distress.

MRS and MRI Data Analyses

We analyzed MRS data using LCModel software version 6.3-1L (37), which performs automatic quantitation of in vivo proton MR spectra as linear combinations of model metabolite spectra (Fig. 2). We report absolute metabolite concentrations in mmol/kg wet weight of brain tissue (see Supplementary Material for details). We applied the following MRS quality control criteria: Spectra with full width at half maximum >10 Hz, signal-to-noise ratio (as measured by LCModel) <10, and full width at half maximum changes by condition >3 Hz were discarded. We then estimated concentrations of all metabolites with Cramér-Rao lower bound (CRLB) ≤10% over all groups and conditions. The metabolites glutamate, Glx, NAA, and TCr remained after exclusion criteria were applied. The low cutoff point of 10% for the CRLB reliability measure was selected to be sensitive to small changes in metabolite values. We performed statistical analyses on glutamate to focus on our main hypothesis concerning effects of acute hyperglycemia on glutamatergic metabolism as well as on NAA as a control metabolite. Group and condition effects on Glx and TCr are explored in the Supplementary Material.

We analyzed rs-fMRI data using the FSL (https://fsl.fmrib.ox.ac.uk) and DPARSF (www.rfmri.org/DPARSF) software packages to calculate the fractional amplitude of low-frequency fluctuations in slow-4 band (fALFF4) (from 0.027 to 0.073 Hz) and slow-5 band (fALFF5) (from 0.001 to 0.027 Hz) of the rs-fMRI time series BOLD signal fluctuations (38,39), which have been proposed to reflect the regional intensity of spontaneous neuronal activity of two distinct sets of oscillators (40) preferentially localized in gray matter (41). For details see the Supplementary Material.

Clinical Depression Symptom Assessments

All subjects underwent psychiatric assessment, including the structured clinical interview for DSM-IV to determine the absence of Axis I disorders. The 17-item Hamilton Depression Rating Scale (HAM-D) was used to assess subjects' depressive symptoms. All subjects also completed the Symptom Checklist-90 Revised (SCL-90-R), consisting of 90 items, which assesses a broad range of symptoms of psychopathology, including depression. The depression rating subscores were extracted from the SCL-90-R for analyses.

Emotional Function Assessments

All subjects performed the computerized version of emotional tasks implemented on a laptop computer (Dell Latitude E6530) using the software package Presentation
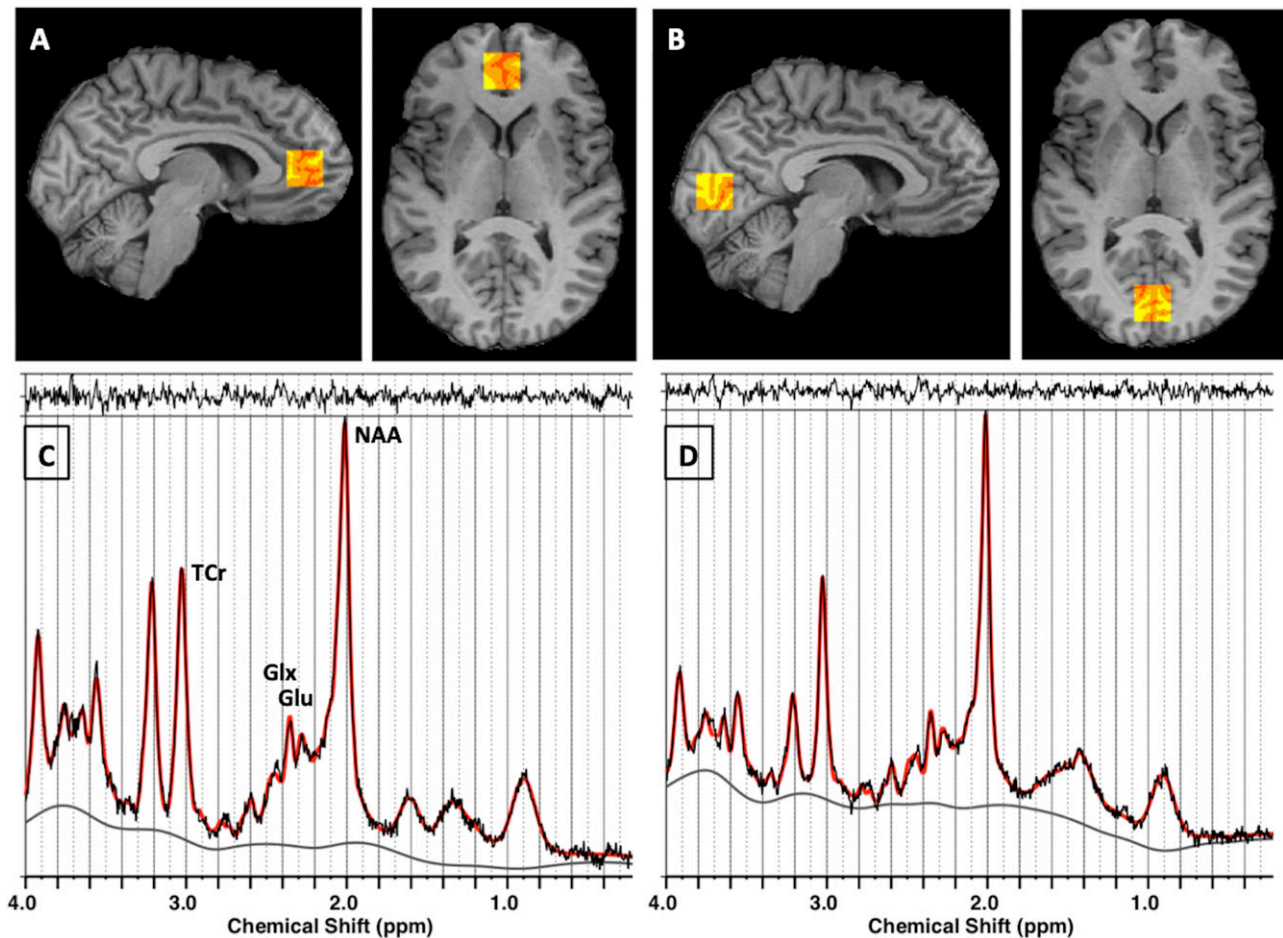
Figure 2—MRS: localization of voxels and spectra analyzed using LCModel. *A* and *B*: Red-yellow scale boxes overlaid on a subject's T1-weighted image in gray scale on sagittal (left) and axial (right) slices show the voxel regions where MRS data were acquired. The colors show the result of the brain tissue segmentation inside the voxel as follows: red, cerebrospinal fluid; orange, gray matter; and yellow, white matter. *A*: Pregenual ACC. *B*: OCC. *C* and *D*: In vivo point-resolved spectroscopy data are shown in black; the LCModel fit to data is shown in red. The top margin shows the residual to the fit, and the bottom line is the spectral baseline fit. *C*: Pregenual ACC. *D*: OCC. Glu, glutamate.

(Neurobehavioral Systems). For these tasks, longer response times to emotionally valued words reflect longer emotional processing time associated with depressive symptoms.

SRET
In the SRET (42), preselected adjectives are presented visually to subjects who then make a categorical decision about whether the word is self-descriptive. The subjects respond by pressing a no or yes response key, and the time between presentation of the word and key press response is recorded. A total of 72 words, including 24 words of each of three types of depression-related emotional valence (affect)—negative (e.g., burdened), positive (e.g., joyful), or neutral (e.g., golfer)—are presented in random order.

Emotional Stroop Task
In the emotional Stroop task (43,44), the subject is asked to name the color in which a word is presented on the screen as quickly as possible while ignoring the meaning of the word. The words have negative or neutral affect and

are presented in red, yellow, green, or blue, with each color occurring equally often with each word's affect category. The subject responds by key press, with one key for each color. Error rates and response times are recorded. A total of 80 words, including 40 with negative affect (e.g., hopeless) and 40 words of neutral affect (e.g., locate), are presented.

Cognitive Assessments
All subjects completed a standard battery of cognitive tests, including the Wechsler Abbreviated Scale of Intelligence (WASI) (45) to measure intelligence quotient (IQ), the abbreviated Delis-Kaplan Executive Function System (D-KEFS) (46) to measure executive function (trail making and verbal fluency), the Wechsler Memory Scale III to measure memory, and the Grooved Pegboard to measure psychomotor speed.

Statistics
Statistical analyses were performed using JMP Pro version 14.0.0 (SAS Institute) and Stata 16 (StataCorp) software.

Metabolites, fALFF, and plasma glucose and insulin levels were analyzed using a linear mixed-effects model with group (T1D or control) and condition (EU or HG period) as fixed effects and subjects as a random effect. Group metabolite (glutamate and NAA) and fALFF changes from EU to HG and group averages during EU or HG were contrasted within the linear model using a t test. Group differences in clinical data and emotional test response times were analyzed using one-way ANOVA with a significance threshold of $P = 0.05$. Pearson correlation coefficients were calculated by bivariate linear fitting to assess the relationship between metabolite concentration changes and emotional test response times. A partial Bonferroni correction was performed on the significance threshold (corrected $P = 0.039$ for uncorrected $\alpha = 0.05$) to account for multiple comparisons and the high correlation of glutamate levels with NAA levels across groups and regions in the mixed-effects model.

Data and Resource Availability
All data generated or analyzed during this study are included in the published article (and its online Supplementary Material). No applicable resources were generated or analyzed during the current study.

RESULTS
Subjects
The subjects' demographic and clinical characteristics are shown in Table 1. The T1D and control groups were well matched for age, sex, years of education, and general cognition and psychomotor skills as evaluated by cognitive (IQ, executive function, memory) and psychomotor (Grooved Pegboard) tests.

Plasma Glucose and Insulin
Plasma glucose levels are shown in Fig. 1. During EU, plasma glucose was 6.1 ± 0.2 mmol/L in the T1D group compared with 5.2 ± 0.2 mmol/L in the control group ($P = 0.006$). During HG, plasma glucose was 11.8 ± 0.2 mmol/L in T1D compared with 10.7 ± 0.2 mmol/L in control ($P = 0.001$) (Fig. 1). There was no significant difference in the increase in plasma glucose from EU to HG between T1D (5.7 ± 0.2 mmol/L) and control (5.5 ± 0.3 mmol/L, $P = 0.594$), and the increase for each group was close to the target value of 5.5 mmol/L.

There was a significant group–by–glycemic condition interaction effect on plasma insulin ($P = 0.0007$). The increase in plasma insulin from EU to HG in the control group (27 ± 4 µU/mL, $P < 0.0001$) was higher than the increase in the T1D group (7 ± 4 mmol/L, $P = 0.080$), which did not reach significance. During EU, plasma insulin was comparable in both groups, with 8 ± 3 µU/mL in T1D compared with 5 ± 3 µU/mL in control ($P = 0.523$). During HG, plasma insulin was 14 ± 3 µU/mL in T1D compared with 33 ± 3 µU/mL in control ($P = 0.0003$). Note that in the control group, the increase in plasma insulin levels is the natural physiological response to the increased infusion of glucose during the clamp, while in the T1D group, plasma insulin was being infused at a constant rate of 0.25 mU/kg/min.

Brain Metabolite Concentrations by MRS
Brain metabolite concentrations in healthy control subjects were comparable to values found in the literature for healthy individuals using similar 3T MRS acquisition and analysis methods (47) as well as those found at higher field strengths (48). Baseline EU concentrations of metabolites in the ACC were higher than those in the OCC (Table 2 and Supplementary Table 2). Instrumental factors, such as radiofrequency field inhomogeneity or spatial variation in coil sensitivity, as well as biological factors, such as brain tissue metabolite and water relaxation times, subjects' age, the difference in ratios of gray matter to white matter between the ACC and OCC voxels in this study (see Supplementary Material), and the reported higher concentrations of glutamate in voxels with more gray than white matter (48), could potentially have contributed to the observed metabolite concentration differences between frontal and occipital lobe voxels.

Glutamate
In the ACC, there was a significant condition-by-group interaction effect for glutamate ($P = 0.035$), while there was no group, condition, or interaction effect for this metabolite in the OCC (Table 2 and Fig. 3). In the T1D group, ACC glutamate increased significantly during the HG (to 13.5 ± 2.0 mmol/kg) compared with EU (12.3 ± 0.9 mmol/kg, $P = 0.014$), while in the control group, it remained unchanged (12.8 ± 1.6 vs. 12.6 ± 1.6 mmol/kg for EU vs. HG, respectively, $P = 0.578$). Thus, the change in ACC glutamate from EU to HG (ΔGlu) was significantly different in T1D (1.2 mmol/kg, +10%) compared with control (-0.2 mmol/kg, -2%, $P = 0.035$). Glutamate was reliably determined over all subjects and conditions as indicated by CRLBs averaging 7% (range 5–10%) in the ACC and 6% (range 5–8%) in the OCC (see Supplementary Table 1).

NAA
There was a significant group effect for NAA in the OCC ($P = 0.008$). OCC NAA concentrations were higher in the T1D group than in the control group during both EU (7.8 ± 0.4 vs. 7.5 ± 0.3 mmol/kg in T1D vs. control, respectively, $P = 0.007$) and HG (7.7 ± 0.4 vs. 7.5 ± 0.2 mmol/kg brain in T1D vs. control, respectively, $P = 0.135$) (Table 2 and Fig. 3). NAA was reliably determined over all subjects and conditions as indicated by CRLBs averaging 4% (range 3–6%) in the ACC and 3% (range 3–5%) in the OCC (see Supplementary Table 1).

Other Metabolites
In an exploratory analysis, we tested group and condition effects on Glx and TCr. For Glx in both regions, there were no significant overall group or condition effects, but there was a trend for a condition-by-group interaction effect in the ACC ($P = 0.049$). There was a significant Glx increase during HG in the T1D group (1.4 mmol/kg, 9%, $P = 0.016$) compared with the control group (-0.3 mmol/kg, -2%, $P = 0.663$). For TCr, there was a significant condition-by-group interaction effect in the ACC ($P = 0.009$). There was

Table 2—Concentrations of metabolites and fALFF in pregenual ACC and OCC during EU and HG

	T1D group				Control group				Linear mixed-effects model P		
	EU (n = 13)	HG (n = 13)	HG – EU	Contrast P	EU (n = 11)	HG (n = 11)	HG – EU	Contrast P	Group	Condition	Condition × group
ACC											
Metabolite											
Glu	12.3 ± 0.9	13.5 ± 2.0	1.2	**0.014**	12.8 ± 1.6	12.6 ± 1.1	−0.2	0.578	0.706	0.194	**0.035**
NAA	8.9 ± 1.1	9.4 ± 1.1	0.5	0.043	8.9 ± 1.1	8.9 ± 1.2	0.0	0.971	0.575	0.154	0.170
Activity index											
fALFF4	0.36 ± 0.04	0.36 ± 0.05	0.00	0.449	0.39 ± 0.03	0.34 ± 0.02	−0.05	**0.002**	0.274	**0.004**	0.061
OCC											
Metabolite											
Glu	7.9 ± 0.6	7.8 ± 0.8	−0.1	0.401	7.4 ± 0.7	7.7 ± 0.8	0.3	0.266	0.242	0.750	0.164
NAA	7.8 ± 0.4	7.7 ± 0.4	−0.1	0.389	7.5 ± 0.3	7.5 ± 0.2	0.0	0.608	**0.008**	0.875	0.345
Activity index											
fALFF4	0.41 ± 0.03	0.43 ± 0.04	0.02	0.196	0.44 ± 0.04	0.42 ± 0.04	−0.02	0.088	0.656	0.667	**0.033**

Data are mean ± SD unless otherwise indicated. Metabolite concentrations are in units of mmol/kg wet weight brain tissue; activity index values are ratios. P values are from the linear mixed-effects model, with main effects of group, condition, and condition × group interaction and contrasts between HG and EU for each group. P values that meet the partial Bonferroni-corrected threshold for significance (P = 0.039) appear in boldface type. Glu, glutamate; HG – EU, change from EU to HG in mmol/kg wet weight brain tissue (mean).
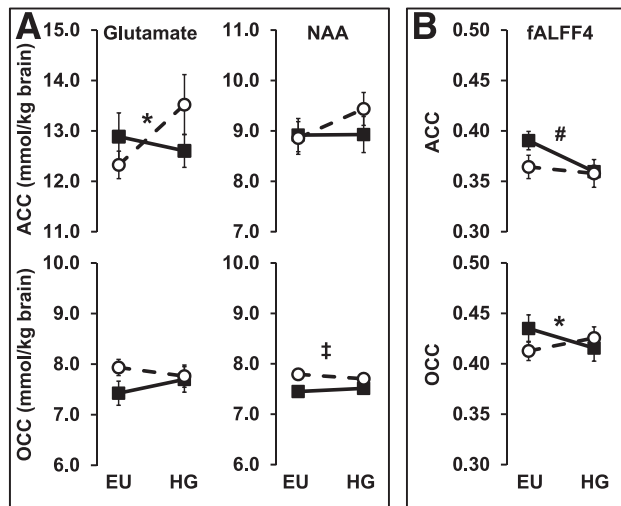
Figure 3—Effects of hyperglycemia on brain metabolites and ALFFs. Mean concentrations of brain metabolites (mmol/kg wet weight brain tissue) (A) and fALFF4 (0.027–0.073 Hz) (B) in ACC and OCC during EU and HG conditions. Open circles and dotted lines represent subjects with T1D; filled squares and solid lines represent control subjects. *Condition-by-group interaction effect; #condition effect; ‡group effect; all P values <0.039 (partial Bonferroni-corrected threshold for significance).

a significant TCr increase during HG in T1D (0.4 mmol/kg, 6%, $P = 0.008$) compared with control (−0.2 mmol/kg, −3%, $P = 0.277$), similar to the pattern of effect on glutamate (see Supplementary Table 2).

Intrinsic Neuronal Activity by fMRI

In the ACC, there was a significant overall condition effect ($P = 0.004$) and a trend for a condition-by-group interaction effect ($P = 0.061$) for fALFF4. There was a significant decrease in ACC fALFF4 during HG in the control group (−0.050, −13%, $P = 0.002$) and no change in the T1D group (−0.007, −2%, $P = 0.449$). In the OCC, there was a significant condition-by-group interaction effect ($P = 0.033$). There was a trend for a decrease in OCC fALFF4 during HG in the control group (−0.02, −5%, $P = 0.088$), while there was no change in the T1D group (0.020, 5%, $P = 0.196$).

Depression Symptoms

The average HAM-D score was significantly higher in subjects with T1D (1.8 ± 1.9) than in healthy control subjects without diabetes (0.3 ± 0.4, $P = 0.020$) (Table 1 and Fig. 4). The average SCL-90-R depression rating subscore was significantly higher in the T1D group (7.3 ± 6.9) than in the control group (1.1 ± 1.5, $P = 0.008$) (Table 1 and Fig. 4). All scores for clinical ratings were below the range for clinical depression, as expected by exclusion criteria for the T1D and control groups.

Emotional Function Tests

The average response time of self-referencing to negative-valence words in the SRET was significantly longer in the

T1D group (1,290 ± 61 ms) than in the control group (1,055 ± 67 ms, $P = 0.017$) (Fig. 4). The average response time in the emotional Stroop task was not significantly different in T1D (888 ± 32 ms) compared with control (827 ± 33 ms, $P = 0.204$) (Fig. 4).

Correlations of ACC Glutamate Changes With Emotional Assessment Scores and Clinical Characteristics

We explored the relationship between ACC glutamate metabolism and emotional processing as well as clinical characteristics of T1D using Pearson correlation. Linear regression analysis of the emotional Stroop response times revealed a tendency for a group-by-ΔGlu interaction ($P = 0.091$). There was a tendency for a positive correlation between the ACC ΔGlu with the emotional Stroop response times to all words in the T1D group (Pearson $r = 0.553$, $P = 0.078$) but not in the control group (0.183, $P = 0.590$) (Fig. 5). There was no significant correlation between ΔGlu and the age of onset of diabetes (−0.355, $P = 0.258$) or between ΔGlu and the duration of diabetes (0.401, $P = 0.197$) in T1D.

DISCUSSION

Our study showed that acute hyperglycemia increased pregenual ACC glutamate concentrations in subjects with T1D compared with age-, education-, and cognition-matched healthy control subjects without diabetes. None of the subjects had current or a prior episode of clinical major depression. The anomalous hyperglycemic glutamate increase was not a global brain effect because no change was seen in the occipital lobe control region of the brain. The association of increased ACC glutamate with acute hyperglycemia in T1D compared with control suggests that the metabolic control of glutamate levels during resting-state ACC neural activity is disrupted in these patients.

Glutamate is the main excitatory neurotransmitter. Its highest concentrations in brain tissue are in neuronal synaptic vesicles (14). In healthy adults, there is a 1:1 linear relationship between the glucose oxidation rate and the glutamate-glutamine cycling rate, which is tightly linked to neurotransmission (13). Glutamate concentrations at the synapse are tightly regulated by complex mechanisms involving astrocytic and neuronal pathways to avoid the risk for neurotoxicity with excessive extracellular levels. For the healthy control subjects in our study, ACC and OCC glutamate levels remained constant during the HG period. The increased availability of glucose in the ACC during acute hyperglycemia did not significantly change the glutamate pool size, suggesting that synaptic neurotransmitter glutamate levels also remained constant within the euglycemic resting-state activity range. This is consistent with a regional brain tissue–level multicellular and multicompartmental regulation of glutamate concentrations—glutamate homeostasis—operating under a steady state of increased glucose availability.

In healthy adults, the resting-state brain glutamate pool concentration remains constant because of a dynamic equilibrium of input and output fluxes with high kinetic rates,
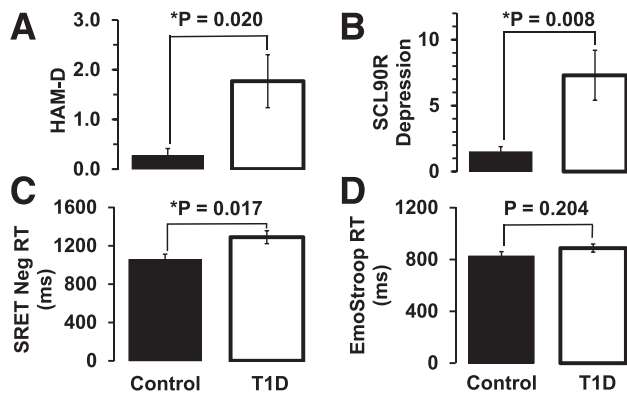
Figure 4—Clinical depression rating and emotional function scores (mean ± SE). *A*: HAM-D rating scores. *B*: SCL-90-R depression rating scores. *C*: SRET negative (Neg)-valence word response times (RT) (ms). *D*: Emotional Stroop (EmoStroop) color-naming response times (ms). *P < 0.05 by one-way ANOVA.

consistent with glutamate's fast-acting excitatory neurotransmitter role. Because glutamate does not cross the blood-brain barrier, it is synthesized in brain tissue from carbon moieties, which are directly or indirectly provided by plasma glucose entering the brain, and its synthesis is matched by its degradation or removal (49). The glutamate level may increase during task-related activation (50) and may also reflect the region's neural engagement in sensory, cognitive, or emotional processing during a given state (51). Thus, increased glutamate during hyperglycemia in T1D could possibly be explained by increased excitatory activity in the ACC. Increased ACC activity in T1D might reflect abnormally increased emotional or cognitive processing in response to an increased glycemic level compared with control. In a study of MDD, resting-state medial prefrontal neuronal activity (measured by ALFF) was shown to positively correlate with medial prefrontal glutamate concentrations, which, in turn, positively correlated with Hamilton anxiety scores (52). However, ACC neuronal activity did not change during HG in T1D. Since control subjects responded to HG with a decrease in fALFF4, the sustained euglycemic levels of neuronal activity during HG in T1D could reflect the absence of a normal emotional or cognitive response to acute hyperglycemia. Also, since increased neuronal activity does not account for the increased glutamate, this suggests instead a disruption of ACC glutamate metabolism. In T1D, in the likely absence of changed glutamate-glutamine cycling during HG (suggested from the absence of changed resting-state neuronal activity), the glutamate increase could occur by perturbed glutamate production or removal in the mitochondrial tricarboxylic acid energetic pathway. Besides the changes in the glutamate pool related to glutamate-glutamine cycling, glutamate production occurs by transamination of α-ketoglutarate, a key component of the tricarboxylic acid cycle, and removal occurs by the opposite reaction for oxidative energy production. Such energetics-related production/removal imbalances in glutamate metabolism would

likely affect task-related glutamatergic activity of emotional or cognitive processing in the ACC of patients with T1D.

In T1D, metabolic adaptations to chronic hyperglycemia, increased availability of glucose, and large glycemic excursions could disrupt glutamate metabolism, resulting in excessive unsynchronized or inefficient neural activity in the ACC, compatible with the observed longer emotional task response times and increased depressive symptoms. Chronic hyperglycemia could upregulate glucose utilization pathways, and frequent hypoglycemic episodes could upregulate alternate substrate utilization (53), with both mechanisms favoring increased glutamate synthesis during acute hyperglycemia. Without commensurate removal by glutamate-glutamine cycling or degradation by mitochondrial oxidation, an increased glutamate pool could result. The current findings are compatible with our previous findings of increased working memory task activation during hypoglycemia in T1D for equivalent levels of performance, which also suggests inefficient neural processing in T1D (18).

Because the ACC continues to develop through adolescence and beyond, the abnormal ACC glutamate changes could possibly be related to glucose dyshomeostasis during critical periods of ACC development. Since no significant correlation was found between ACC glutamate changes and age of diabetes onset, it is unlikely that development of the brain significantly contributes to the observed effect in T1D in this study. However, the negative association (i.e., younger age at onset related to greater glutamate change) suggests that a study of a larger sample might demonstrate a clinically meaningful relationship.

An unexpected finding was that OCC NAA was significantly higher in the T1D group than in the control group during both euglycemia and hyperglycemia. NAA, synthesized in the mitochondria, indexes neuronal energetic viability related to mitochondrial function. Thus, chronic hyperglycemia may upregulate mitochondrial energetic pathways or increase mitochondrial or synaptic density in the OCC of patients with T1D. Since glutamate oxidation for energetic production occurs in mitochondria, this could allow for increased glutamate removal and could explain why OCC glutamate does not increase in T1D during HG. The lack of group effect on NAA in the ACC also suggests that such mitochondrial function upregulation does not occur in the ACC of patients with T1D. The increased OCC NAA finding in our study is contrary to the decreased occipital lobe NAA levels found in chronic T1D by Mangia et al. (30). This discrepancy could be explained by the differences in age and diabetes duration between the two studies. The study by Mangia et al. comprised middle-aged patients (age 41 ± 11 years) with long diabetes duration (22 ± 12 years), while our study comprised younger patients (age 25 ± 4 years) with shorter diabetes duration (13 ± 6 years). Thus, our results could indicate an early compensatory mechanism to sustain neural processing, which could eventually break down with longer durations of diabetes and poor glycemic control. A regional compensatory mechanism was also invoked
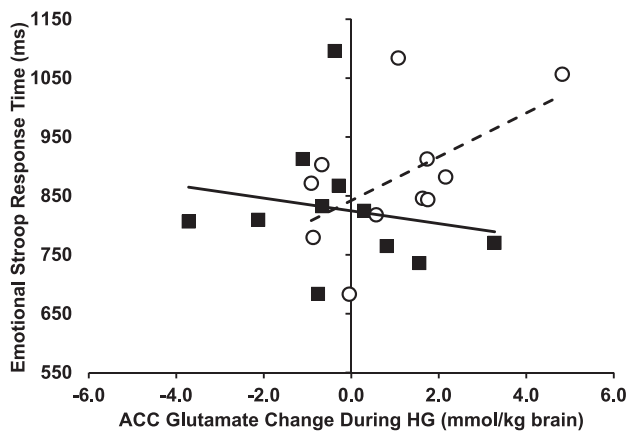
Figure 5—Emotional Stroop response time vs. ACC glutamate change during HG. Plot of response times vs. ACC ΔGlu concentration from euglycemia to hyperglycemia (mmol/kg wet weight brain tissue). Open circles represent T1D; filled squares represent controls. The dotted line represents the linear fit to the T1D data points (Pearson $r = 0.553$, $P = 0.078$). The solid line represents the linear fit to the control data points (Pearson $r = 0.183$, $P = 0.590$). Increased color-naming response times tended to associate with increased ACC ΔGlu for subjects with T1D only (group-by-ΔGlu interaction effect $P = 0.091$).

to explain higher task activation associated with better performance in the parietal lobe and with worse performance in the frontal lobe in an fMRI study of T1D (32).

An unexpected exploratory finding was the significant condition-by-group interaction effect for TCr in the ACC. ACC TCr concentrations followed a pattern similar to that of glutamate concentrations, increasing during HG in the T1D group with no change in the control group and no effect in OCC. TCr is the cell's energetic buffer, allowing regeneration of ATP after its use in cellular processes, such as spiking activity in neurons or macromolecule synthetic activity. Since brain creatine synthesis (which occurs in mitochondria) is limited, levels are mostly maintained by active transport from the serum (54). Increased TCr could allow for increased ATP-consuming activity during HG in T1D. Rapid increases in TCr during acute hyperglycemia could reflect early alterations in regional brain energetic metabolism in T1D.

Our study assessed ALFF, which measures the intensity of BOLD fluctuations at specific low-frequency bands and reflects the intensity of coherent neural activity involved in neural processing (55). Changes in unsynchronized neuronal activity would not be reflected by these measures. Excessive glutamate levels result in unregulated stimulation of N-methyl-D-aspartate receptors, which are believed to constitute the conditions to elicit a cascade of excitation-mediated neuronal damage where excessive increases in intracellular calcium concentrations finally trigger neuronal damage and apoptosis. Also, reduction of glutamatergic synapses could result from an adaptation to excessive levels of glutamate by plasticity mechanisms (56). The observed increased glutamate levels without concomitant increases in coherent neural

activity suggest that unregulated neuronal activity could be occurring in the ACC and its connected neural networks during HG. Thus, early dysregulation in glutamatergic activity during acute hyperglycemic episodes could explain later prefrontal cortical thinning observed in T1D (25).

In both the emotional Stroop task and the SRET, emotional bias is measured by the tendency for participants to exaggerate or misperceive negative emotional information, which leads to increased response times. Response times to the emotional Stroop task tended to positively correlate with the hyperglycemic ACC glutamate change in subjects with T1D only. Subjects performed the emotional Stroop task several days before the MRS assessments during baseline glycemic levels, which likely would have been higher in T1D and highest in T1D with poor control. The positive relationship suggests that longer response times are associated with greater disruption of ACC glutamate metabolism. In an fMRI study, patients with MDD had longer response times and showed higher ACC task-related functional activity compared with control subjects, and ACC functional activity was positively correlated with response times (27). Our results are similar and suggest that the disrupted glutamate homeostasis reflects abnormal glutamatergic activity related to an emotional bias toward negative thoughts. The longer SRET negative word response times in T1D further support that self-reference emotional processing is perturbed in these patients potentially because of abnormal activity in ACC-associated emotional processing networks.

Finally, clinical depressive symptom rating scores were significantly higher in the T1D group than in the control group, while remaining at a level below that of a depressive episode. None of the subjects from either group reported any discomfort or concern during scanning; this suggests that stress from the HG was not a confounding factor contributing to differences in ACC glutamate. Overall, our results suggest that abnormal ACC glutamatergic neurotransmission could affect emotional processing in T1D.

No subjects in this study had ever experienced a major depressive episode, which precludes the effect of a major depressive episode on the observed glutamate metabolic perturbation. Thus, the glutamate perturbation may be an early sign of dysregulated glutamatergic function that could worsen with worse or longer periods of poor glycemic control. Sustained excessive or incoherent glutamatergic activity during hyperglycemia could damage neurons by excitotoxicity or synaptic plasticity mechanisms, with further disruption of ACC-associated brain networks.

Our study was limited by the use of single-voxel MRS, which limited our investigation to the pregenual ACC and a control visual occipital lobe region. Thus, we could not infer any metabolite changes in other brain regions, which could potentially be more relevant to emotional processing or self-referencing. Furthermore, we were limited by the use of a high-field 3T scanner as opposed to an ultra-high-field 7T scanner that may have provided higher sensitivity,

spectral resolution, and reliability for estimation of metabolite concentrations. MRS acquisitions did not allow reliable determination of GABA levels; thus, we were unable to examine the role of GABA levels and metabolism and excitatory/inhibitory balance in this study. Caution is needed for the interpretation of our absolute metabolite levels, their relative ratios, and comparisons of these variables in our study with those of other MRS studies. The scanner (57), head coil, MRS acquisition and analysis methods, voxel location, metabolite relaxation times, and subject age may impact the variance of metabolite concentration estimates. However, these experimental factors should not overly affect the interpretation of our results relative to our primary hypothesis, which was based on the comparison of glutamate concentrations between euglycemic and hyperglycemic conditions, with other experimental conditions remaining constant or controlled. Also, the small number of subjects in each group may have limited the statistical power.

If high glycemic levels during long periods of time and acute hyperglycemic episodes contribute to excessive pregenual ACC glutamate and abnormal glutamatergic activity as our study suggests, then emotional or cognitive prefrontal function may worsen with longer durations of poor glycemic control, ultimately contributing to a major depressive episode. Current standard treatments targeting improved glucose control should limit the development of such glutamatergic dysfunction. Our study further suggests that medications targeting glutamatergic neurotransmission pathways may be particularly effective to treat depression in T1D. Furthermore, early adjunct glutamatergic treatments may limit or prevent the development of depression in T1D and exert a neuroprotective effect.

References

1. Roy T, Lloyd CE. Epidemiology of depression and diabetes: a systematic review. J Affect Disord 2012;142(Suppl.):S8–S21
2. Barnard KD, Skinner TC, Peveler R. The prevalence of co-morbid depression in adults with Type 1 diabetes: systematic literature review. Diabet Med 2006;23:445–448
3. Gilsanz P, Karter AJ, Beeri MS, Quesenberry CP, Whitmer RA. The bi-directional association between depression and severe hypoglycemic and hyperglycemic events in type 1 diabetes. Diabetes Care 2018;41:446–452
4. Stoeckel LE, Arvanitakis Z, Gandy S, et al. "White Paper" meeting summary and catalyst for future inquiry: complex mechanisms linking neurocognitive dysfunction to insulin resistance and other metabolic dysfunction. F1000 Res 2016;5:353
5. Anderson RJ, Freedland KE, Clouse RE, Lustman PJ. The prevalence of comorbid depression in adults with diabetes: a meta-analysis. Diabetes Care 2001;24:1069–1078
6. Magistretti PJ, Pellerin L, Rothman DL, Shulman RG. Energy on demand. Science 1999;283:496–497
7. Amidfar M, Woelfer M, Réus GZ, Quevedo J, Walter M, Kim Y-K. The role of NMDA receptor in neurobiology and treatment of major depressive disorder: evidence from translational research. Prog Neuropsychopharmacol Biol Psychiatry 2019;94:109668
8. Contractor A, Heinemann SF. Glutamate receptor trafficking in synaptic plasticity. Sci STKE 2002;2002:re14
9. Trudeau F, Gagnon S, Massicotte G. Hippocampal synaptic plasticity and glutamate receptor regulation: influences of diabetes mellitus. Eur J Pharmacol 2004;490:177–186
10. Bar-Peled O, Ben-Hur H, Biegon A, et al. Distribution of glutamate transporter subtypes during human brain development. J Neurochem 1997;69:2571–2580
11. Lodge D, Watkins JC, Bortolotto ZA, Jane DE, Volianskis A. The 1980s: D-AP5, LTP and a decade of NMDA receptor discoveries. *Neurochem Res* 2019;44:516–530
12. Simonyi A, Schachtman TR, Christoffersen GRJ. The role of metabotropic glutamate receptor 5 in learning and memory processes. Drug News Perspect 2005;18:353–361
13. Shulman RG, Hyder F, Rothman DL. Biophysical basis of brain activity: implications for neuroimaging. Q Rev Biophys 2002;35:287–325
14. Zhou Y, Danbolt NC. Glutamate as a neurotransmitter in the healthy brain. J Neural Transm (Vienna) 2014;121:799–817
15. Bolo NR, Renshaw PF. Magnetic resonance spectroscopy. In *Essentials of Neuroimaging for Clinical Practice*. Dougherty DD, Rauch SL, Rosenbaum JF, Eds. Washington DC, London, England, American Psychiatric Publishing, Inc, 2004, p. 105–116
16. Lyoo IK, Yoon SJ, Musen G, et al. Altered prefrontal glutamate-glutamine-gamma-aminobutyric acid levels and relation to low cognitive performance and depressive symptoms in type 1 diabetes mellitus. Arch Gen Psychiatry 2009;66:878–887
17. Luykx JJ, Laban KG, van den Heuvel MP, et al. Region and state specific glutamate downregulation in major depressive disorder: a meta-analysis of (1)H-MRS findings. Neurosci Biobehav Rev 2012;36:198–205
18. Bolo NR, Musen G, Jacobson AM, et al. Brain activation during working memory is altered in patients with type 1 diabetes during hypoglycemia. Diabetes 2011;60:3256–3264
19. Bolo NR, Musen G, Simonson DC, et al. Functional connectivity of insula, basal ganglia, and prefrontal executive control networks during hypoglycemia in type 1 diabetes. J Neurosci 2015;35:11012–11023
20. Zhou M, Hu X, Lu L, et al. Intrinsic cerebral activity at resting state in adults with major depressive disorder: a meta-analysis. Prog Neuropsychopharmacol Biol Psychiatry 2017;75:157–164

21. Moriguchi S, Takamiya A, Noda Y, et al. Glutamatergic neurometabolite levels in major depressive disorder: a systematic review and meta-analysis of proton magnetic resonance spectroscopy studies. Mol Psychiatry 2019; 24:952–964

22. Gerhard DM, Wohleb ES, Duman RS. Emerging treatment mechanisms for depression: focus on glutamate and synaptic plasticity. Drug Discov Today 2016; 21:454–464

23. McEwen AM, Burgess DTA, Hanstock CC, et al. Increased glutamate levels in the medial prefrontal cortex in patients with postpartum depression. Neuropsychopharmacology 2012;37:2428–2435

24. Godlewska BR, Masaki C, Sharpley AL, Cowen PJ, Emir UE. Brain glutamate in medication-free depressed patients: a proton MRS study at 7 Tesla. Psychol Med 2018;48:1731–1737

25. Lyoo IK, Yoon S, Jacobson AM, et al. Prefrontal cortical deficits in type 1 diabetes mellitus: brain correlates of comorbid depression. Arch Gen Psychiatry 2012;69:1267–1276

26. Vogt BA. Submodalities of emotion in the context of cingulate subregions. Cortex 2014;59:197–202

27. Mitterschiffthaler MT, Williams SCR, Walsh ND, et al. Neural basis of the emotional Stroop interference effect in major depression. Psychol Med 2008;38: 247–256

28. Sacher J, Neumann J, Fünfstück T, Soliman A, Villringer A, Schroeter ML. Mapping the depressed brain: a meta-analysis of structural and functional alterations in major depressive disorder. J Affect Disord 2012;140:142–148

29. Tolomeo S, Christmas D, Jentzsch I, et al. A causal role for the anterior midcingulate cortex in negative affect and cognitive control. Brain 2016;139:1844–1854

30. Mangia S, Kumar AF, Moheet AA, et al. Neurochemical profile of patients with type 1 diabetes measured by ^{1}H-MRS at 4 T. J Cereb Blood Flow Metab 2013;33: 754–759

31. Wiegers EC, Rooijackers HM, van Asten JJA, et al. Elevated brain glutamate levels in type 1 diabetes: correlations with glycaemic control and age of disease onset but not with hypoglycaemia awareness status. Diabetologia 2019;62:1065–1073

32. Hwang M, Tudorascu DL, Nunley K, et al. Brain activation and psychomotor speed in middle-aged patients with type 1 diabetes: relationships with hyperglycemia and brain small vessel disease. J Diabetes Res 2016;2016: 9571464

33. Diabetes Control and Complications Trial Epidemiology of Diabetes Interventions and Complications Study Research Group. Effects of intensive diabetes therapy on neuropsychological function in adults in the Diabetes Control and Complications Trial. Ann Intern Med 1996;124:379–388

34. DeFronzo RA, Tobin JD, Andres R. Glucose clamp technique: a method for quantifying insulin secretion and resistance. Am J Physiol 1979;237:E214–E223

35. Ernst T, Kreis R, Ross BD. Absolute quantitation of water and metabolites in the human brain. I. Compartments and water. J Magn Reson B 1993;102:1–8

36. Gasparovic C, Song T, Devier D, et al. Use of tissue water as a concentration reference for proton spectroscopic imaging. Magn Reson Med 2006;55:1219–1226

37. Provencher SW. Estimation of metabolite concentrations from localized in vivo proton NMR spectra. Magn Reson Med 1993;30:672–679

38. Zang Y-F, He Y, Zhu C-Z, et al. Altered baseline brain activity in children with ADHD revealed by resting-state functional MRI. Brain Dev 2007;29:83–91

39. Zou Q-H, Zhu C-Z, Yang Y, et al. An improved approach to detection of amplitude of low-frequency fluctuation (ALFF) for resting-state fMRI: fractional ALFF. J Neurosci Methods 2008;172:137–141

40. Buzsáki G, Draguhn A. Neuronal oscillations in cortical networks. Science 2004;304:1926–1929

41. Zuo X-N, Di Martino A, Kelly C, et al. The oscillating brain: complex and reliable. Neuroimage 2010;49:1432–1445

42. Dobson KS, Shaw BF. Specificity and stability of self-referent encoding in clinical depression. J Abnorm Psychol 1987;96:34–40

43. Williams JMG, Mathews A, MacLeod C. The emotional Stroop task and psychopathology. Psychol Bull 1996;120:3–24

44. Compton RJ, Banich MT, Mohanty A, et al. Paying attention to emotion: an fMRI investigation of cognitive and emotional Stroop tasks. Cogn Affect Behav Neurosci 2003;3:81–96

45. Wechsler D. *Wechsler Abbreviated Scale of Intelligence WASI Manual.* New York, Psychological Corporation, 1999

46. Delis DC, Kaplan E, Kramer JH. *Delis-Kaplan Executive Function System: Examiner's Manual.* New York, The Psychological Corporation, 2001

47. Tarumi R, Tsugawa S, Noda Y, et al. Levels of glutamatergic neurometabolites in patients with severe treatment-resistant schizophrenia: a proton magnetic resonance spectroscopy study. Neuropsychopharmacology 2020;45: 632–640

48. van den Bogaard SJA, Dumas EM, Teeuwisse WM, et al. Exploratory 7-Tesla magnetic resonance spectroscopy in Huntington's disease provides in vivo evidence for impaired energy metabolism. J Neurol 2011;258:2230–2239

49. Sonnewald U. Glutamate synthesis has to be matched by its degradation - where do all the carbons go? J Neurochem 2014;131:399–406

50. Mangia S, Giove F, Dinuzzo M. Metabolic pathways and activity-dependent modulation of glutamate concentration in the human brain. Neurochem Res 2012; 37:2554–2561

51. Lynn J, Woodcock EA, Anand C, Khatib D, Stanley JA. Differences in steady-state glutamate levels and variability between 'non-task-active' conditions: evidence from ^{1}H fMRS of the prefrontal cortex. Neuroimage 2018; 172:554–561

52. Zhang X, Tang Y, Maletic-Savatic M, et al. Altered neuronal spontaneous activity correlates with glutamate concentration in medial prefrontal cortex of major depressed females: an fMRI-MRS study. J Affect Disord 2016;201: 153–161

53. Mason GF, Petersen KF, Lebon V, Rothman DL, Shulman GI. Increased brain monocarboxylic acid transport and utilization in type 1 diabetes. Diabetes 2006;55: 929–934

54. Kious BM, Kondo DG, Renshaw PF. Creatine for the treatment of depression. Biomolecules 2019;9:406

55. Tomasi D, Volkow ND. Association between brain activation and functional connectivity. Cereb Cortex 2019;29:1984–1996

56. Citri A, Malenka RC. Synaptic plasticity: multiple forms, functions, and mechanisms. Neuropsychopharmacology 2008;33:18–41

57. van de Bank BL, Emir UE, Boer VO, et al. Multi-center reproducibility of neurochemical profiles in the human brain at 7 T. NMR Biomed 2015;28:306–316